

Contents lists available at ScienceDirect

Polymer

journal homepage: www.elsevier.com/locate/polymer



An infection-responsive collagen-based wet-spun textile fibre for wound monitoring

Jonathon Gorman a,b, Charles Brooker b, Xinyu Li, Giuseppe Tronci b, fo

- a Clothworkers Centre for Textile Materials Innovation for Healthcare (CCTMIH), Leeds Institute of Textiles and Colour (LITAC), University of Leeds, United Kingdom
- ^b Division of Oral Biology, St. James's University Hospital, School of Dentistry, University of Leeds, United Kingdom

ARTICLE INFO

Keywords:
Collagen fibre
Wet spinning
Infection monitoring
Wound dressing
Bromothymol blue
pH indicator

ABSTRACT

Wound infections are a significant clinical and socioeconomic challenge, contributing to delayed healing and increased wound chronicity. To enable early infection detection and inform therapeutic decisions, this study investigated the design of pH-responsive collagen fibres using a scalable wet spinning process, evaluating product suitability for textile dressings and resorbable sutures. Type I collagen was chemically functionalised with 4-vinylbenzyl chloride, enabling UV-induced crosslinking and yielding mechanically robust fibres. Bromothymol blue, a halochromic dye responsive to pH changes, was incorporated via drop-casting to impart visual infection-responsive colour change. Gravimetric analysis and Fourier Transform Infrared Spectroscopy confirmed high dye loading, whereby a Loading Efficiency of 99 \pm 3 wt% was achieved. The fibres exhibited controlled swelling in aqueous environments (Swelling Ratio: $323 \pm 79 - 492 \pm 73$ wt%) and remarkable wet-state Ultimate Tensile Strength (UTS: 12±3-15 ± 7 MPa), while up to ca. 30 wt% of their initial crosslinked mass was retained after 24 h in a collagenase-rich buffer (pH 7.4, 37 °C, 2 CDU) and ethanol series dehydration. Importantly, distinct and reversible colour transitions were observed between acidic (pH 5) and alkaline (pH 8) environments, with up to 88 wt% dye retention following 72-h incubation. The fibres were successfully processed into woven dressing prototypes and demonstrated knotting ability suitable for suture applications. Overall, these wet-spun collagen fibres integrate infection-responsive capability, biodegradability, and scalable fabrication, representing a promising platform for smart wound dressings and resorbable sutures.

1. Introduction

Wound infections remain a major clinical challenge, contributing significantly to delayed healing, prolonged hospital visits, and increased healthcare costs worldwide. In severe cases, infected wounds can lead to sepsis and require limb amputation [1]. The cost of treating wounds in the UK alone was estimated to be £8.8 billion in 2022 [2], and in the US, this figure approaches \$150 billion [3]. Conventional methods for diagnosing wound infections, such as microbial swabbing, tissue biopsies, and visual inspection, are often invasive, slow to yield results, expensive, or subjective [4]. These shortcomings have prompted an increased interest in non-invasive, real-time biomarkers that can signal infection progression at earlier stages.

One promising biomarker of wound infection is local pH, which undergoes characteristic changes during wound progression. Monitoring wound pH is a key indicator for predicting bacterial infections and assessing the stages of wound healing. Healthy skin typically

exhibits an acidic pH (\approx 4–6) [5], which is associated with the production of lactic acid; this acidic pH environment is beneficial for enhancing fibroblast proliferation, angiogenesis, and collagen synthesis towards wound healing [6]. On the other hand, infected wounds become increasingly alkaline due to the destruction of the extracellular matrix (ECM) and the release of ammonia, leading to an increased wound alkalinity (pH > 7) [7]. Consequently, several wound monitoring technologies have emerged to address this need, including electrochemical sensors [8], colorimetric assays [9], and optical probes [10].

While promising, many of these 'smart' wound monitoring systems still need to overcome technical challenges. For example, conventional glass-based electrochemical sensors used to monitor pH are often mechanically fragile [11], and fluorometric methods often lack long-term stability and require the use of a UV lamp [12,13]. Ion-sensitive field-effect transistors (ISFETs) represent another class of electrochemical pH sensors [14]; however, concerns remain regarding their relatively high operating voltage and limited sensitivity [15]. The widespread

^{*} Corresponding author. Level 7 Wellcome Trust Brenner Building, St. James's University Hospital, Leeds, LS9 7TF, United Kingdom. E-mail address: g.tronci@leeds.ac.uk (G. Tronci).

clinical adoption of these smart wound dressings remains limited, largely due to factors such as high cost, lack of disposability, and bulkiness, which hinder their seamless integration into conventional dressings [16]. Moreover, the design complexity presents additional barriers to clinical translation, including regulatory approval and user compliance [17], highlighting the need for simple, robust designs that are both scalable and clinically viable.

Type I collagen is the most abundant protein of connective tissues in the human body and widely recognised for its biocompatibility, biodegradability, and low immunogenicity. These characteristics make it one of the most deployed biomaterials in commercially available wound care products, including wound dressings and surgical sutures, due to its wound healing and inherent bioactive properties. Type I collagen helps to simulate the native microenvironment of a wound and aids in promoting cell proliferation, differentiation, and migration, which is essential for stimulating the synthesis of new ECM and attracting fibroblasts to the wound bed [18–20]. Building on the advantages of textile-based wound care platforms, including wound dressings and sutures, type I collagen fibres present an ideal biodegradable substrate to support wound healing.

Unlike purely synthetic textiles, type I collagen degrades enzymatically (via collagenases), releasing chemotactic peptides that can promote angiogenesis and tissue remodelling [21-23]. Additionally, the presence of reactive side-chains allows for chemical functionalisation [24], potentially enabling the integration of structural support, real-time sensing, and/or controlled therapeutic release within a single, biocompatible platform. The limited solubility of type I collagen in organic solvents also makes it compliant with scalable fibre manufacturing techniques, i.e. wet spinning, aiming to accomplish individual fibres as building block of fibrous materials. On the other hand, the uncontrollable water-induced swelling of type I collagen ex vivo present significant challenges towards the successful delivery of collagen-based materials at industrial scale. To overcome these issues, there is a crucial need to develop multiscale design approaches that enable control of molecular scale and microscale in collagen-based materials aiming to meet key functional requirements and usability needs.

Many commercial wound dressings are made from textile fibres due to their inherent flexibility and mechanical strength [25–27]. By embedding responsive elements directly into fibres, smart textiles can provide real-time feedback on wound status while maintaining breathability and a close, non-disruptive interface with the wound bed [28]. In addition to dressings, textile fibres can also be integrated into sutures, which are in direct and prolonged contact with tissue, offering a valuable platform for real-time monitoring, targeted therapeutic delivery alongside biodegradability, removing the requirement for secondary surgery [29–32]. Utilising scalable manufacturing techniques, such as wet spinning [33] and weaving [34], can support the production of disposable, low-cost devices suitable for clinical translation [35–37].

In our previous work, we developed a pH-responsive collagen-based theranostic dressing made of UV-cured functionalised type I collagen, incorporating bromothymol blue (BTB). The resulting prototype demonstrated cellular tolerability, dye retention over clinically relevant timeframes, and prompt visual infection indication [38]. However, these formats were limited in their integrability with use-inspired clinical functionalities. In this work, we focus on the design of the functionalised collagen product in fibrous form, which offers several practical and translational advantages. To achieve this, we identified wet spinning as a promising, scalable manufacturing route to produce continuous collagen fibres with controlled fibre morphology, thermo-mechanical properties, and UV-cured molecular network architecture, so that their applicability as three-dimensional textiles and resorbable suture was successfully demonstrated. Wet spun functionalised collagen fibres were loaded with BTB via a gravitational drop cast method, allowing the fibres to endow pH-sensitive characteristics for use in textile wound dressings and resorbable sutures. The molecular configuration of BTB enables visual colour changes in response to variations in environmental

pH without the need for clinical equipment or an algorithm. This multiscale design approach aims to overcome limitations observed in collagen-based wound care systems, such as poor fibre integrity in aqueous environments, rapid dye release, and limited handling capability, while supporting the development of smart wound monitoring devices aligned with industrial manufacturing practice and regulatory expectations.

2. Materials and methods

2.1. Materials

Rat tails were provided post-mortem from the School of Dentistry, University of Leeds and used for the extraction of type I collagen via acidic treatment, as described by Rajan et al. [39]. Triethylamine (TEA), ethanol (EtOH), picryl sulfonic acid solution (5 % w/v in water), sodium bicarbonate, calcium chloride, and collagenase from Clostridium histolyticum (125 CDU•mg⁻¹) were purchased from Sigma-Aldrich (Gillingham, UK). A 17.4 M acetic acid (AcOH) solution, and glacial hydrochloric acid (HCl) solution, were also purchased from Sigma-Aldrich and diluted with deionised water before use. 4-vinvlbenzyl chloride (4VBC) was purchased from Thermo Fisher Scientific (Massachusetts, USA). 2-Hydroxy-4'-(2-hydroxyethoxy)-2-methylpro piophenone (I2959) and N-[Tris(hydroxymethyl)methyl]-2-amino ethanesulfonic acid (TES) were purchased from Merck (Feltham, UK). Phosphate-buffered saline (PBS) was purchased from Corning UK (Flintshire, UK). Polysorbate 20 (Tween 20) was purchased from Scientific Laboratory Supplies Ltd (Nottingham, UK). Bromothymol Blue (BTB) was purchased from Alfa Aesar (Heysham, UK).

2.2. Manufacture of collagen fibres

4VBC-functionalised collagen was synthesised as previously reported by Tronci et al. [40]. Briefly, rat tail collagen (CRT) was dissolved in 17.4 mM AcOH and reacted with 25-molar excess of 4VBC and TEA with respect to the molar content of collagen lysines ($\approx 2.7 \times 10^{-4} \, \text{mol} \, \text{eg}^{-1}$). After 24 h, the reaction mixture was precipitated in 10-fold ethanol for 24 h, recovered by centrifugation, and air dried. The resulting 4VBC-functionalised collagen product was dissolved in 17.4 mM AcOH supplemented with 1 wt% I2959 under magnetic stirring for 24 h. The resulting wet-spinning dope was loaded into a 10 mL syringe with an internal diameter of 15.7 mm and equipped with a 1.1 mm (19G) diameter needle. The solution was thoroughly agitated to minimise the risk of air bubbles and mounted onto a syringe pump (World Precision Instruments, Hitchin, UK). Wet spinning was performed at a flow rate of 12.5 mL h^{-1} by immersing the needle into a coagulation bath comprising either EtOH or EtOH supplemented with 0.5-1 wt% I2959, maintained in contact with ice. A thin layer of petroleum jelly was applied to the bottom of the coagulation bath to prevent fibre adhesion. The extruded fibres were left in the coagulation bath for 5-10 min (until they became transparent), followed by 15 min of UV irradiation (1.8 mW cm⁻¹, Chromato-Vue C-71, Analytik Jena, Upland, CA, USA), on both sides. Samples were then dehydrated via a graded distilled water-ethanol series (20, 40, 60, 80, 100 vol% EtOH) prior to air-drying. UV-cured wet-spun collagen fibres were designated as F-4VBC*, where F indicates the fibre format, 4VBC denotes chemical functionalisation, and * indicates the UV-cured, crosslinked state.

2.3. Fibre loading with BTB

A gravimetric method was employed to quantify the loading content of BTB in drop-cast collagen fibres (n = 14). The initial mass of each individual dry sample (m_i) was recorded using a precision five-decimal-place analytical balance (Sartorius, Göttingen, Germany). Subsequently, 100 μ L of a 0.2 wt% BTB solution was added to each sample using a micropipette. After 48 h of air-drying, the final mass (m_f) of the drop-

cast samples was recorded, and the Loading Efficiency (LE) calculated via Eq. (1):

$$LE = \frac{\left(m_f - m_i\right)}{m_{BTB}}$$
 Equation 1

where m_{BTB} is the mass of BTB contained in the volume of the aqueous solution applied to the samples during drop casting. Drop-cast, BTB-loaded fibres were coded as B–4VBC*, where B refers to the fibre encapsulation with BTB, while 4VBC and * have the same meaning as above

2.4. Chemical characterisation

Attenuated total reflectance Fourier-transform infrared (ATR-FTIR) spectroscopy (PerkinElmer Spectrum 3) was employed to assess the chemical composition of the dry samples (n = 3). The FTIR spectra were recorded with a spectral resolution of 4 $\rm cm^{-1}$ and a scan interval of 2 $\rm cm^{-1}$.

2,4,6-Trinitrobenzenesulfonic acid (TNBS) assays were conducted as a colorimetric technique to quantify primary amino groups in proteins [41]. Solutions of 0.5 wt% TNBS and 4 wt% NaHCO₃ were prepared in distilled water. One millilitre of each solution was pipetted onto samples of native and functionalised collagen (11 mg, n = 3). After 4 h of stirring at 40 $^{\circ}$ C, 3 mL of 6 N HCl was added, followed by 1 h of incubation at 60 °C. Following equilibration to room temperature, 5 mL of distilled water was added to all samples. Samples were extracted three times with 20 mL of diethyl ether. Subsequently, 5 mL of the aqueous phase were collected and diluted with 15 mL of distilled water prior to absorbance measurement at 346 nm using a UV-Vis spectrophotometer (Jenway 6305 UV-vis spectrophotometer, Essex, United Kingdom). Blank samples (11 mg) were prepared in the same manner as the test samples, except that 3 mL of 6 N HCl was added together with the TNBS and NaHCO3 solutions prior to incubation at 40 °C. The molar content of collagen lysines and the degree of collagen functionalisation (F) were quantified using Eqs. (2) and (3):

$$\frac{\textit{Mol(lys)}}{\textit{g(collagen)}} = \frac{2 \times \textit{ABS} \times \textit{V}}{\mu \times b \times \textit{m}_d}$$
 Equation 2

$$F = \left(1 - \frac{mol(Lys)_{Funct}}{mol(Lys)_{Native}}\right) \times 100$$
 Equation 3

whereby ABS is the solution absorbance recorded at 346 nm, μ is the molar absorption coefficient of 2,4,6-trinitrophenyl lysine (1.46 \times 10⁴ M⁻¹ cm⁻¹), b is the path length of the cuvette (1 cm), m_d is the mass of the dry sample (11 mg) and V is the volume of solution (0.02 L).

2.5. Thermal analysis

Thermogravimetric analysis (TGA) and differential scanning calorimetry (DSC) were performed to assess the thermal properties of dry BTB-free and BTB-loaded collagen fibres. TGA (PerkinElmer TGA 4000, Massachusetts, USA) was carried out under a nitrogen flow rate of 50 cm 3 min $^{-1}$, starting at 30 $^{\circ}$ C and ramping to 900 $^{\circ}$ C at 10 $^{\circ}$ C \bullet min $^{-1}$. Samples were held at 900 $^{\circ}$ C for 5 min in a nitrogen atmosphere, followed by 1 min in air at the same temperature.

DSC (PerkinElmer DSC 4000, Massachusetts, USA) was performed on dehydrated samples (n = 3, $\approx \! 10$ mg). Thermograms were recorded from $-10~^{\circ}\text{C}$ to $150~^{\circ}\text{C}$ at a heating rate of $10~^{\circ}\text{C} \bullet \text{min}^{-1}$. Prior to measurement, the DSC cell was calibrated using indium as the standard under a nitrogen flow rate of $50~\text{cm}^3~\text{min}^{-1}$.

2.6. Optical and electron microscopy

Light microscopy (Leica M205C) was used to measure the thickness of dehydrated and rehydrated fibres (n = 10), with rehydration

performed in PBS for 10 h. Fibre morphology was examined in the dry state using scanning electron microscopy (SEM; Hitachi SU3900, Hitachi, Tokyo, Japan) under high vacuum mode. Prior to imaging, all samples were gold-coated using a sputter coater (Emscope SC500, Emscope, Ashford, United Kingdom).

2.7. Quantification of linear density

The dry mass (m_d) of the fibre samples was measured (Ohaus Discovery DV314C, New Jersey, USA), while their length (I) was measured with a universal tensile machine (Instron 5544-Massachusetts, USA). The linear density of the fibres (λ, tex) was then calculated using Eq. (4):

$$\lambda = \frac{m_d}{l} \times 1000$$
 Equation 4

2.8. Swelling ratio and gel content measurements

The dry mass (m_d) of BTB-free and BTB-loaded fibres was recorded using an analytical balance (Ohaus Discovery DV314C, New Jersey, USA). Samples were then incubated in deionised water (DI) for 2 h. After incubation, swollen samples were gently blotted on filter paper, and the swollen mass (m_s) was recorded. The swelling ratio (SR) was calculated using Eq. (5):

$$SR = \frac{m_s - m_d}{m_d} \times 100$$
 Equation 5

In addition, the gel content (G) of the fibres (n = 3) was quantified as an indirect measurement of the crosslink density of the respective UV-cured molecular network. Dry samples of known mass (m_d) were incubated in 17.4 mM AcOH for 24 h. Following incubation, the samples were collected and dried through a graded ethanol-distilled water series before measuring the resulting mass (m_e). G was then calculated using Eq. (6):

$$G = \frac{m_e}{m_d} \times 100$$
 Equation 6

2.9. Tensile testing of hydrated fibres

The tensile properties of the individual BTB-free and BTB-loaded collagen fibres were assessed after incubation in PBS for 2 h, using an Instron 5544 (Massachusetts, USA) at a temperature of 20 ± 2 °C and a relative humidity of 65 ± 4 % (n =5). The fibres had a gauge length of 20 mm, the crosshead speed was 2 mm min $^{-1}$, and tests were conducted using a 5 N load cell. The Young's modulus was calculated using the linear region of the stress-strain curve.

2.10. In vitro studies of dye release

The dye retention in the drop-cast collagen fibres was indirectly assessed by measuring the dye release following sample incubation in aqueous environments. McIlvaine solutions adjusted to either pH 5 or pH 8 were selected to simulate active and infected wound environments, respectively [5]. Individual collagen fibres (n = 3), loaded with either 100 μg or 60 μg of BTB, were incubated in 5 mL of the aforementioned acidic and alkaline McIlvaine solutions, respectively, at room temperature. The release of BTB in each solution was determined over 4 days by measuring the absorbance of the buffer solution via UV–Vis spectrophotometry (Jenway 6305 UV–vis spectrophotometer, Essex, United Kingdom). Calibration curves were built by dissolving known amounts of BTB in a McIlvaine solution adjusted to either pH 5 or pH 8 (Fig. S1, Supp. Inf.), with absorbance recorded at 432 nm and 616 nm, respectively. The resulting calibration curves were used to quantify the BTB released over time.

2.11. Colorimetric analysis

The colour of the fibres was recorded using an SF600 Plus-CT spectrophotometer (Datacolor, Lucerne, Switzerland), following UV curing, drop casting, or 96-h incubation in either pH 5 or pH 8 McIlvaine solution. After calibration against standard black and white standards, the lightness, chroma, and hue were measured using a 3-mm aperture. Three replicates were tested for each sample type, with three individual measurements taken per replicate (n = 9). Results were reported as mean \pm standard deviation.

2.12. Enzymatic degradation tests

Collagenase from Clostridium histolyticum (125 CDU·mg⁻¹) was employed to assess the enzymatic degradation of BTB-loaded collagen fibres in vitro, in accordance with previous reports [31,42]. Bovine type I collagen was used to fabricate UV-cured wet-spun fibres, due to its high purity and comparable chemical composition to rat tail collagen [43] (Fig. S2, Supp. Inf.). Dry BTB-loaded fibres (m_d: 10–20 mg; BTB: 60 μg) were incubated in a 1 mL of collagenase-rich buffer (50 mM TES, 0.36 mM calcium chloride, pH 7.4; 2 CDU•mL⁻¹) under mild agitation (150 rpm, 37 °C). The value of collagenase concentration was calculated according to Equations S1 and S2 (Supp. Inf.). Enzymatic degradation studies were also performed on native rat tail collagen, UV-cured rat tail collagen fibres, and UV-cured rat tail collagen thin films, following incubation in 5 mL of a collagenase-rich buffer (50 mM TES, 0.36 mM calcium chloride, pH 7.4; 0.4 CDU•mL⁻¹) under mild agitation (150 rpm, 37 °C). At selected time points, samples were collected, washed in distilled water and dehydrated through a graded distilled water-ethanol series (0, 20, 40, 60, 80, 100 vol% EtOH) before air-drying. The dry mass of the retrieved samples (m_t) was recorded, and the relative mass (μ_{rel}) calculated using Eq. (7):

$$\mu_{rel} = \frac{m_t}{m_d}$$
 Equation 7

where m_t represents the mass of the dry sample at the incubation time t; m_d represents the samples mass prior to incubation.

2.13. Fibre weaving and suturing trials

To demonstrate the fibre usability in textile wound dressings, three UV-cured fibres were twisted into yarns, and the yarns spliced to reach a suitable length for further processing. Hand weaving was subsequently carried out to generate a textile wound dressing prototype.

For suture application, individual UV-cured fibres were secured to suture needles (3-0 20 mm 1/2c) to produce single knots, alongside a commercially available silk-braided, non-absorbable suture control.

2.14. Statistical analysis

OriginPro 2024b was used to perform statistical analysis and plotting of the experimental data visualisation. Normality was assessed by the Shapiro-Wilk test, followed by one-way ANOVA to evaluate statistical significance (p < 0.05). Data are expressed as mean \pm standard deviation.

3. Results and discussion

3.1. Chemical characterisation

The degree of functionalisation in 4VBC-reacted collagen samples was quantified via a TNBS colorimetric assay and found to be 33 ± 3 mol.% (Table S1, Supp. Inf.), in line with previous reports [31]. This result indicates successful covalent attachment of 4VBC residues onto the lysine side chains and amino termini of collagen. This modification

constitutes a critical step towards the formation of a covalently crosslinked network of collagen molecules upon subsequent UV irradiation.

The results of the TNBS assay were complemented by FTIR analysis to characterise the chemical composition of the wet-spun collagen fibres, following either UV exposure or BTB loading. Distinct amide bands were identified in the FTIR spectrum of native type I collagen control (Fig. 1A), including: (i) amide A and B at 3300 and 3080 cm^{-1} respectively, indicative of N-H stretching vibrations; (ii) amide I and II bands, at 1630 and 1540 cm⁻¹, corresponding to C=O stretching vibrations, and N-H bending and C-N stretching vibrations, respectively; and (iii) an amide III band centred at 1240 cm⁻¹, attributed to the C-N stretching and N-H bending vibrations of amide linkages, as well as wagging vibrations of CH2 groups in the glycine backbone and proline side chains. These characteristic signals were also observed in the FTIR spectra of the wet-spun fibres (Fig. 1B and C), confirming their collagenbased chemical composition, whereby the detection of the amide III band at 1240 cm⁻¹ supports the presence of the triple helical configuration of type I collagen [44].

The absorbance ratio of the amide III band to the one at $1450~\rm cm^{-1}$ ($A_{\rm III}/A_{1450}$) was subsequently measured across the collagen control and wet-spun samples to provide further insight into the protein structure within the fibres. A value close to unity was observed in native collagen and UV-cured wet-spun fibres ($A_{\rm III}/A_{1450}=0.97-1.02$), indicating preservation of the triple helix configuration, consistent with the minimal impact of the selected wet spinning and UV curing process on the collagen molecules [40,45,46]. In contrast, BTB-loaded collagen samples exhibited a slightly lower absorbance ratio ($A_{\rm III}/A_{1450}=0.89$), suggesting partial loss of the collagen triple helices following BTB drop casting. Similar observations have previously been recorded with cast

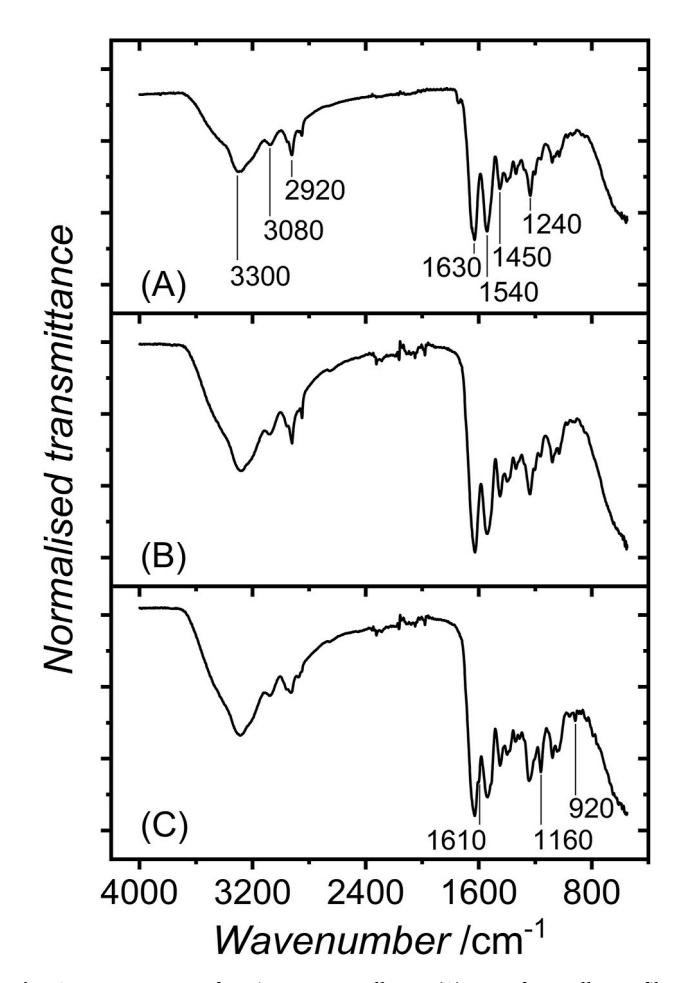


Fig. 1. FTIR spectra of native type I collagen (A), BTB-free collagen fibre F-4VBC* (B), and BTB-loaded fibre B-4VBC* (C).

films of the same collagen composition [38] and may be attributed to functional groups in the BTB molecule potentially interfering with the secondary interactions that stabilise the collagen triple helix. This hypothesis is supported by the appearance of an additional shoulder at 1610 cm⁻¹ in the FTIR spectra of B-4VBC* compared to F-4VBC*, indicative of secondary interactions between the aromatic rings of 4VBC-functionalised collagen molecules and BTB in the dry state.

In addition to the collagen signals, further bands were detected in the FTIR spectrum of the BTB-loaded sample (Fig. 1C), specifically at 1160 and 920 cm $^{-1}$, which were assigned to C—O stretching vibrations and aromatic C–H bending vibrations in BTB, respectively [47]. These observations are supported by gravimetric analysis performed on the same samples, which revealed a weight increase and a BTB loading efficiency of 99 \pm 3 wt% following drop casting (n = 14; Table S2, Supp. Inf.). These results therefore confirm the validity of the selected drop-casting method as a compelling, low-cost and effective technique to accomplish BTB-loaded wet-spun fibres with a high loading efficiency. While we have previously demonstrated the preparation of BTB-loaded cast films (\varnothing : 10–15 mm) [38], these results provide further evidence that this BTB encapsulation strategy is also effective with samples of textile fibres with significantly decreased diameter ($\varnothing \ll 1$ mm).

3.2. Wet spinning of photoactive collagen fibres

Wet spinning of 4VBC-functionalised collagen was performed by dissolving the product in a 17.4 mM AcOH solution supplemented with I2959 (1 wt%), with the aim of producing photoinitiator-containing wetspun fibres suitable for subsequent UV curing. Given the high solubility of I2959 in ethanol, varying concentrations of the photoinitiator were introduced to the ethanol-based coagulation bath to minimise the risks of photoinitiator diffusion away of the fibre-forming collagen jet. The photoinitiator retention in the fibres was considered crucial due to the direct influence of I2959 concentration on crosslink density, gel content, and mechanical properties of photoinduced hydrogel networks [31,48,49]. UV–Vis measurements were therefore conducted on the coagulation bath before and after collagen dope extrusion to quantify any soluble factor release occurring following the wet spinning process (Table S3, Supp. Inf.).

Control experiments performed with I2959-free collagen dope and I2959-free coagulation bath showed a post-spinning increase in the bath absorbance (Abs: $0.000 \rightarrow 0.005$), indicating a slight accumulation of the 4VBC-functionalised collagen product in the bath. A further negligible increase in solution absorbance (Abs: $0.000 \rightarrow 0.007$) was measured following the extrusion of the I2959-supplemented collagen dope (1 wt% I2959) into the I2959-free coagulation bath. Taking into account the relatively low absorbance values (Abs <0.1) and the potential for light interference [50], these UV-Vis readings suggest that a marginal fraction of functionalised collagen originally present in the dope is released to the coagulation bath, i.e. it does not contribute to fibre formation, alongside a small fraction of I2959 that is leached from the fibre-forming dope to the bath. The significant retention of the photoinitiator within the wet-spun fibres is likely attributable to the development of secondary interactions, such as hydrogen bonding or aromatic interactions, between 4VBC-functionalised collagen and 12959.

The minimal photoinitiator diffusion observed during the spinning process is also consistent with the improved handleability exhibited by the UV-cured collagen fibres (in comparison to their non-cured counterparts). This was mostly observed following coagulation in an ethanol bath supplemented with 0.5 wt% I2959, whereby no increase in post-spinning bath absorbance was recorded (Table S3, Supp. Inf.), suggesting that the reduced photoinitiator concentration gradient between the dope and the bath contributed delayed soluble factor diffusion away from the dope. These wet spinning conditions were therefore adopted for the fabrication of wet-spun collagen fibres and subsequent fibre characterisation.

3.3. Fibre morphology

Following confirmation of the chemical composition, attention was directed towards investigating the fibre morphology in the wet-spun samples. Optical microscopy revealed the formation of homogeneous individual fibres in both the UV-cured and drop-cast states (Fig. 2A–D), with fibre diameters of 173 \pm 52 μm (n = 352), respectively. A linear density of 5 \pm 1 tex was measured for fibres in the natural relaxed state.

Fibre loading with BTB resulted in slightly smaller, though statistically insignificant, fibre diameters, likely due to hydrogen bonding effects following drop casting and solvent evaporation. In contrast, larger fibre diameters were observed following sample incubation in aqueous environments, consistent with the water-induced swelling behaviour of type I collagen.

Closer inspection of the fibre morphology by SEM revealed a longitudinally striated fibre structure (Fig. 2E–H), attributed to a relatively high viscosity of the collagen wet-spinning solution [51], and the formation of physical interactions between collagen-grafted 4VBC residues [46], ultimately generating uneven shear forces during the wet-spinning process [52]. The dimensional variations observed in drop-cast samples by light microscopy were corroborated by SEM (Fig. 2H), where local reductions in fibre diameter were detected, most likely arising from the effect of solvent evaporation following drop casting and molecular reorganisation of collagen molecules via hydrogen bonding.

Overall, these investigations demonstrate the manufacturability of 4VBC-functionalised collagen into textile fibres. Nonetheless, further optimisation of the wet-spinning parameters and process remains necessary to achieve improved control over fibre morphology, fineness, and length.

3.4. Thermal behaviour

Previous investigations of chemical composition and fibre morphology were subsequently complemented by thermal analysis, aimed at assessing the impact of BTB loading on the thermal properties of the wet-spun collagen fibres. TGA indicated increased thermal stability for the BTB-loaded (B–4VBC*), in comparison to BTB-free (F–4BC*), fibres (Fig. 3A).

The BTB-loaded samples exhibited a remaining mass of 20 ± 2 wt% at $800\,^{\circ}\text{C}$, compared to <1 wt% in the BTB-free samples. Compared to F–4VBC*, the drop-cast fibres displayed more rapid mass loss below $230\,^{\circ}\text{C}$, while enhanced mass retention was observed at higher temperatures. Upon comparison of the TGA profiles beyond water evaporation (T $>100\,^{\circ}\text{C}$), the first linear decrease in mass was noted in the range of $250–350\,^{\circ}\text{C}$ for F–4VBC* (mass loss ≈30 wt%), comparable to other type I collagen samples [53]. In contrast, this transition occurred at a higher temperature and within a narrower temperature range in the drop-cast samples (T: $300–350\,^{\circ}\text{C}$), whereby approximately half of the mass loss ($\approx16\,$ wt%) was recorded relative to F–4VBC*. As the decomposition temperature of BTB has been reported to be approximately $230\,^{\circ}\text{C}$ [54], these observations support the encapsulation of BTB within the fibres, in agreement with the preceding FTIR (Fig. 1) and gravimetric loading efficiency results.

In addition to TGA, DSC thermograms of dry BTB-free and BTB-loaded fibres revealed a single endothermic transition at 86 ± 5 °C and 91 ± 6 °C, respectively (Fig. 3B and Table 1). This observation is consistent with previous reports on dry covalently crosslinked type I collagen [55] and is attributed to the denaturation of collagen triple helices into random coils [40,46,56]. This result further supports the presence of collagen triple helices within the wet-spun fibres, while the slight, though statistically insignificant, increase in denaturation temperature (Td) in the dry samples of B–4VBC* samples compared to variants F–4VBC* correlates with the formation of secondary interactions between BTB and the collagen network at the molecular level.

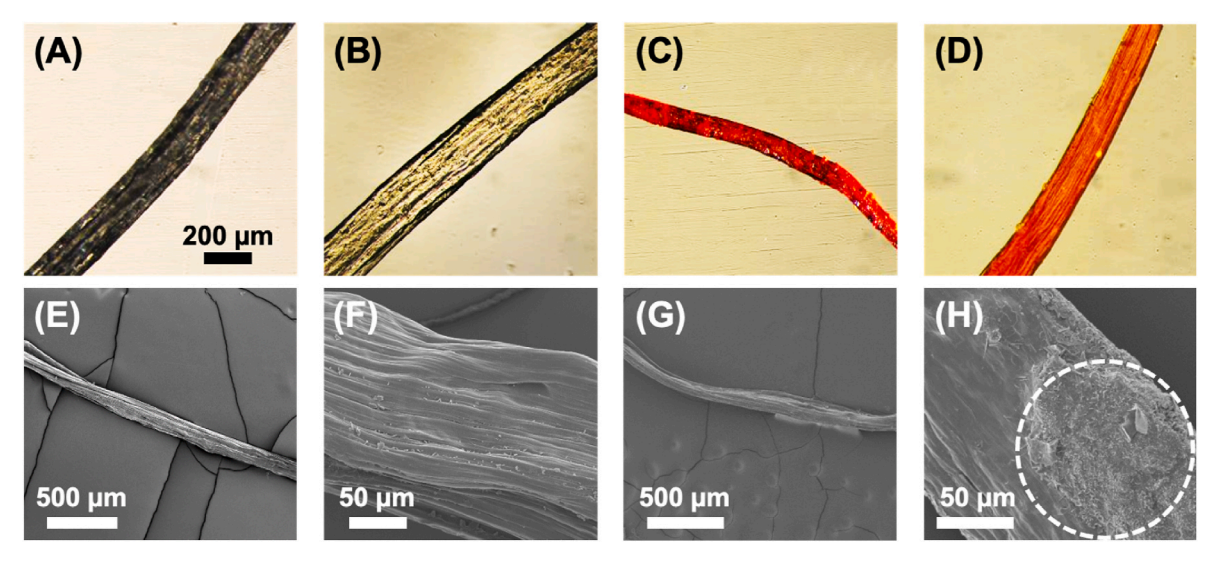


Fig. 2. Morphology of UV-cured wet spun collagen fibres. (A–D): Optical images of BTB-free (A–B) and BTB-loaded (C–D) fibres in the dry (A, C) and hydrated (B, D) states. Scale bar applies to all images. (E–H): Electron microscopy images of BTB-free (E–F) and BTB-loaded (G–H) fibres. The dashed white circle highlights a localised BTB drop cast region of reduced fibre diameter, most likely arising from solvent evaporation effects following drop-casting.

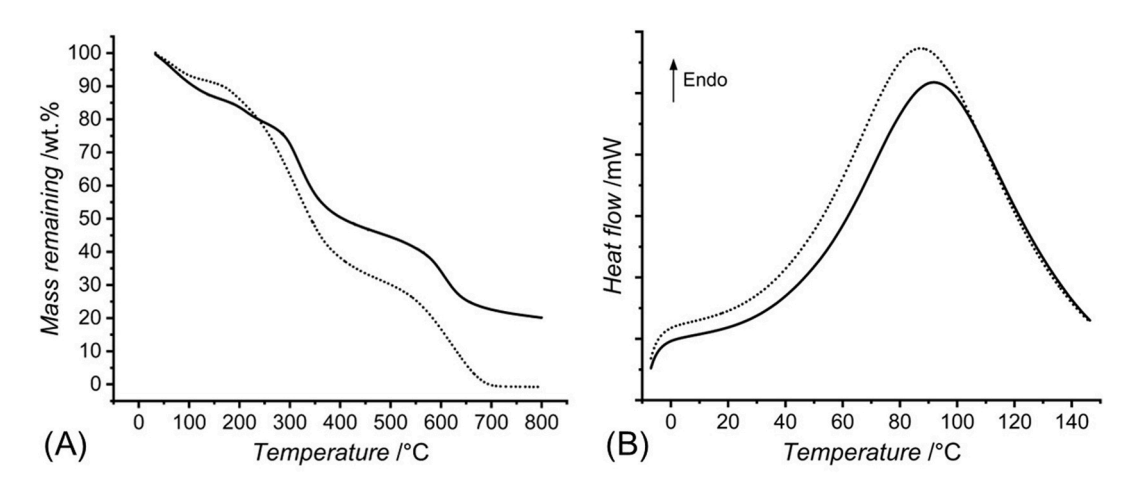


Fig. 3. Representative TGA (A) and DSC (B) thermograms of BTB-loaded (solid line) and BTB-free (dotted line) UV-cured wet-spun collagen fibre.

Table 1 Thermal, swelling, and wet-state mechanical properties of BTB-free and BTB-loaded fibres determined by weight, DSC and tensile measurements, respectively. T_d : denaturation temperature; SR: equilibrium swelling ratio in distilled water; UTS: ultimate tensile strength; ϵ_b : elongation at break; E: tensile modulus; G: gel content. Three replicates were employed for each measurement except for tensile testing, whereby five replicates were measured for each sample. N/A: not applicable.

Sample ID	T _d (°C)	SR (wt. %)	UTS (MPa)	ε _b (%)	E (MPa)	G (wt. %)
F-4VBC* F-4VBC*B	$\begin{array}{c} 86\pm 5 \\ 91\pm 6 \end{array}$	$492\pm73\\323\pm79$	$\begin{array}{c} 15\pm7 \\ 12\pm3 \end{array}$	$\begin{array}{c} 14 \pm 4 \\ 17 \pm 5 \end{array}$	$\begin{array}{c} 232\pm32 \\ 265\pm51 \end{array}$	81 ± 6 N/A

3.5. Characterisation of physical properties

Following the characterisation of the dry fibres, attention turned to sample testing in aqueous environments, with the aim of assessing macroscopic properties and infection responsivity in use-inspired conditions. The mean swelling ratio (SR) recorded at equilibrium after 2 h of incubation in deionised water was 492 ± 73 wt% and 323 ± 79 wt% for BTB-free and BTB-loaded fibres, respectively (Table 1). The slightly lower, though statistically insignificant, SR observed following fibre

encapsulation with the dye aligns with the formation of secondary interactions between the dye and the collagen network, as indicated by the slight increase in T_d (Fig. 3B) and the appearance of an additional shoulder peak in the FTIR spectrum (Fig. 1) of the BTB-loaded samples compared to their BTB-free counterparts.

The aforementioned SR values exhibited by the fibres were significantly lower than those recorded when the same material was processed into cast films [31], which displayed an equilibrium swelling ratio of 1915 \pm 311 wt% under identical experimental conditions. To investigate the origin of this discrepancy, the gel content (G) of the fibres was quantified as an indirect measure of the crosslink density. G values were recorded in the range of 79 ± 6 and 92 ± 1 wt% in samples wet spun into ethanol baths supplemented with varying concentrations of I2959 (Fig. 4).

The gel content data revealed no statistical significance among samples, indicating that the supplementation of the coagulation bath with I2959 had a negligible effect on the crosslink density of the resulting UV-cured wet spun fibres.

This finding indirectly supports earlier UV-Vis absorbance data, which suggested photoinitiator retention within the wet spun fibre following dope extrusion. These UV-Vis data also suggest that the fraction of I2959 released to the coagulation bath did not seem to be

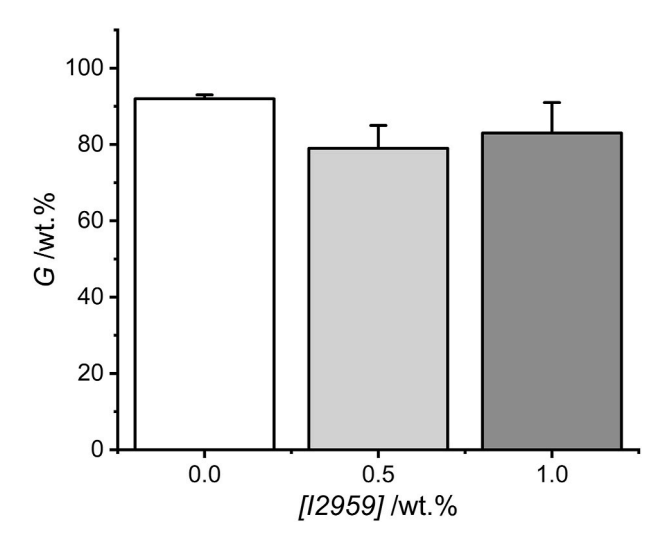


Fig. 4. Gel content (G) exhibited by collagen fibres (n=3) wet spun from an I2959-supplemented collagen dope (1 wt% I2959) in an ethanol bath supplemented with increasing concentration of I2959 (0–1 wt.%) and UV-cured. No significant differences were measured between the three sample groups.

inversely correlated with the observed gel content variation of the resulting UV-cured fibres. This observation possibly hints at the fact that decreased concentration of I2959 in the wet spinning dope compared to the one used in this study (0.5 wt% I2959) may still be sufficient to accomplish comparable crosslink density.

Although no statistically significant differences were observed, the relatively high G values align with earlier reports for comparable cast films [31], suggesting similar crosslink densities and swelling behaviours between the two material formats. However, the significantly reduced SR observed in the fibres compared to their thin film counterparts' points to additional structural factors influencing water uptake. The most logical explanation for the markedly lower SR observed in the fibres, as compared to the films, lies in the wet spinning process itself. During extrusion into the coagulation bath, collagen molecules experience shear and elongation flow, promoting longitudinal alignment and tight molecular packing of the collagen molecules along the fibre axis [46,51,57]. This structural organisation limits the formation of a porous microstructure, thus reducing the free volume and the capacity of the fibres to absorb water. In contrast, cast films allow molecules to adopt a more relaxed and isotropic structural arrangement prior to crosslinking. preserving greater porosity and water-accessible swelling domains. These observations highlight the role of processing-induced microstructure in dictating the functional properties of collagen-based

Despite their significantly reduced swelling compared to thin films, the SR values recorded for the fibres remain comparable to those exhibited by commercial polyurethane-based wound dressings designed to maintain a moist wound environment [43,58]. In this context, the fabrication of individual collagen-based fibres is appealing aiming to meet current industrial practice for the manufacture of fibrous wound dressings, whereby fibre bundles are twisted into yarns and subsequently woven into a three-dimensional porous textile construct. This structural configuration can be beneficial at aiming for enhanced absorption and retention of biological fluids relative to individual fibres. On the other hand, the relatively low SR of the individual fibres may prove advantageous in applications such as resorbable sutures [59].

In addition to the swelling tests, the enzymatic degradability of the wet-spun fibres was assessed, given the rapid cleavage of collagen-based materials *in vivo*. To explore this challenge, UV-cured wet spun fibres were prepared from clinically approved bovine type I collagen and incubated in a collagenase-rich medium (2CDU·mL $^{-1}$) for up to 72 h, followed by ethanol series dehydration [42,43]. Individual fibres

retrieved following 24-h incubation indicated around one third of relative mass ($\mu_{rel}=34\pm14$ wt%), while further mass decrease was observed at 48 h ($\mu_{rel}=11\pm7$ wt%) and 72 h ($\mu_{rel}=11\pm4$ wt%) (Table S4, Supp. Inf.). These trends were confirmed by the rat tail collagen-based variants of wet spun fibre (Fig. 5), while complete degradation of native rat tail collagen was observed within 24 h, in line with the absence of a UV-cured covalent network at the molecular scale. Interestingly, similar values of μ_{rel} were also measured with rat tail collagen thin films, indicating comparable degradation rate of the UV-cured collagen network independently of its processing into fibre or film and respective material size (Fig. 5).

The aforementioned relative mass values revealed by the UV-cured fibres indicate enhanced enzymatic stability compared to commercially available collagen-based membranes and previously reported photocured collagen prototypes. Vallecillo et al. found that Fibro-Gide, Mucograft, and Mucoderm were completely degraded within 48 h under experimental conditions comparable to the ones reported in this study [60]. Similarly, Ali et al. found that UV-cured methacrylated collagen hydrogels lost over 50 % of their mass after only 4 h in a collagenase-supplemented solution (2.5 CDU) [61]. Although the degradation times observed in the present study appear relatively short, it is well established that degradation *in vivo* typically proceeds more slowly than *in vitro*, as physiological conditions are generally less aggressive than the idealised enzymatic environments used in laboratory assays [62].

While the materials tested in this degradation study were completely submerged in the enzymatic medium, further research is warranted to develop clinically relevant degradation models to improve *in vitro* simulations for the *in vivo* applications of the collagen fibres. Degradation studies in these use-inspired environments should include tensile testing at various degradation time points to assess the effect of degradation on mechanical performance and structural integrity [63]. In this context, ensuring material integrity and stability over time is essential to reduce risks of wound exposure to exogeneous bacteria. However, achieving controlled degradation of collagen is a desirable property to foster wound healing in hard-to-heal wounds, whilst also removing the need for secondary surgery in suture applications [32,64].

3.6. Dye release and colour-change capability

Following confirmation of dye loading efficiency and swelling

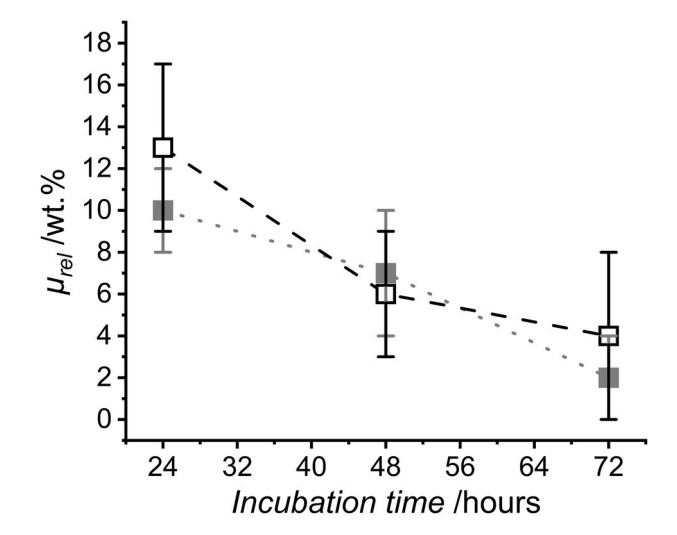


Fig. 5. Temporal profiles of relative mass (μ_{rel}) exhibited by samples (n=3) of UV-cured wet spun fibre $(\cdots \square \cdots)$ and thin film $(\cdots \square \cdots)$ following 72-h incubation in a collagenase-rich medium (2 CDU; pH 7.4; 37°C). Data are presented as mean \pm standard deviation; no significant differences were measured between the two sample groups at each time point.

properties, the colour-change behaviour of the wet-spun collagen fibres was assessed in simulated wound fluids. The fibres were incubated in acidic (pH 5) and alkaline (pH 8) McIlvane buffer solutions for 96 h at room temperature to determine whether dye leaching would occur during a clinically relevant wound dressing application period, as this could irreversibly alter the wound environment and compromise dressing longevity and performance. Testing in vitro was conducted at room temperature to reflect the conditions experienced at the wound-dressing interface, which is typically cooler than core body temperature [65]. The temperature of the chronic wound bed has been reported to be around 33 $^{\circ}$ C, i.e. lower than 37 $^{\circ}$ C, and to be as low as 25.3 $^{\circ}$ C following dressing change. Buffer solutions were adjusted at pH 5 and pH 8 aiming to investigate the pH responsivity of the collagen samples in the most extreme healing and chronic wound environments, respectively, and demonstrate a clear, visually detectable pH-induced colour change. Incubation studies were therefore conducted in the above conditions aiming to investigate the extent of dye retention within the fibres, as a crucial aspect to ensure durable infection responsiveness and to minimise the risk of dressing-induced toxicity.

Following complete submersion of the fibres in acidic McIlvaine buffer (pH 5), negligible dye release was detected in the supernatant, corresponding to a mean value of 12 wt% after 96 h (Fig. 6A–C). The significant retention of the dye in this aqueous environment is most likely due to the development of electrostatic interactions between BTB and the collagen-based fibres (Scheme 1). At pH 5, the negatively charged sulfonate groups of BTB can interact with the protonated amines of the collagen network (pKa \approx 9), consistent with the minimal release previously observed under these conditions [38]. These electrostatic interactions likely complement any $\pi-\pi$ aromatic stacking interactions between BTB and 4VBC-crosslinked collagen molecules, as previously supported by FTIR data (Fig. 1).

In contrast to the acidic environment, a significant increase in dye release was observed following 96-h incubation in alkaline McIlvaine solution (pH 8), rising from 12 ± 2 wt% to 40 ± 4 wt% (Fig. 6A–C). This increase is likely due to the deprotonation of collagen amine groups under alkaline conditions and the resulting electrostatic repulsion of the negatively charged sulfonate groups of BTB and the now neutral or negatively charged collagen network (Scheme 1).

To gain further insight into the release mechanism and test the

aforementioned hypothesis, the release data were fitted using the Korsmeyer-Peppas model (Fig. 6B). The model showed a strong correlation with the release profile observed under alkaline conditions (pH 8), as supported by an \mathbb{R}^2 value of 0.98. The release exponent, n, was measured to be below 1, with a value of 0.236, consistent with a diffusion-controlled release mechanism. In contrast, poorer model fit was observed when applying Korsmeyer-Peppas model to the release data recorded under acidic conditions (pH 5), yielding \mathbb{R}^2 and n values of 0.84 and 0.088, respectively. While the low n value still indicates a diffusion-driven mechanism, the reduced value of \mathbb{R}^2 is likely attributable to the relatively low dye release ([BTB] = 12 ± 2 wt%) after 96 h in the acidic medium.

While the aforementioned testing was carried at room temperature, rather than wound bed temperature (T \approx 33 °C), it is unlikely that a temperature increase in this range would significantly affect the dye release capability of the presented collagen materials, given the presence of a crosslinked network [66] and the lack of thermosensitive segments [67] at the molecular scale.

In our previous work, a two-layer mesh composed of electrospun BTB-encapsulated poly(methyl methacrylate-co-methacrylic acid) (PMMA-co-MAA) fibres displayed BTB release levels of up to 99 wt% after 2 h of incubation in alkaline conditions, while a markedly lower release of 26 wt% was recorded at pH 5 after 96 h [68]. This high release correlates with the absence of ionisable primary amine groups in the PMMA-co-MAA backbone, contrasting with the significantly reduced release observed from the drop-cast UV-cured wet-spun collagen fibres developed in the present study. On the other hand, curcumin-loaded chitosan films were found to release up to ca. 65 wt% of curcumin following 72 h of incubation in aqueous environments. This fraction was reduced to around 40 wt% when the chitosan films were encapsulated with curcumin-loaded silica nanoparticles [69]. Here, lower curcumin release (≈30 wt%) was measured in highly acidic solutions (pH 2) compared to the case of mildly acidic (pH 6) and slightly alkaline (pH 7.4) conditions, an effect attributed to protonation of the primary amino groups of chitosan in acidic media. Similar levels of anthocyanin release (<45 wt%) were also observed when a two-layer composite of agar and carrageenan encapsulated with anthocyanin-loaded liposomes was incubated in aqueous solutions for 70 min, while complete release was recorded in the absence of liposomes [70]. In contrast to these reports,

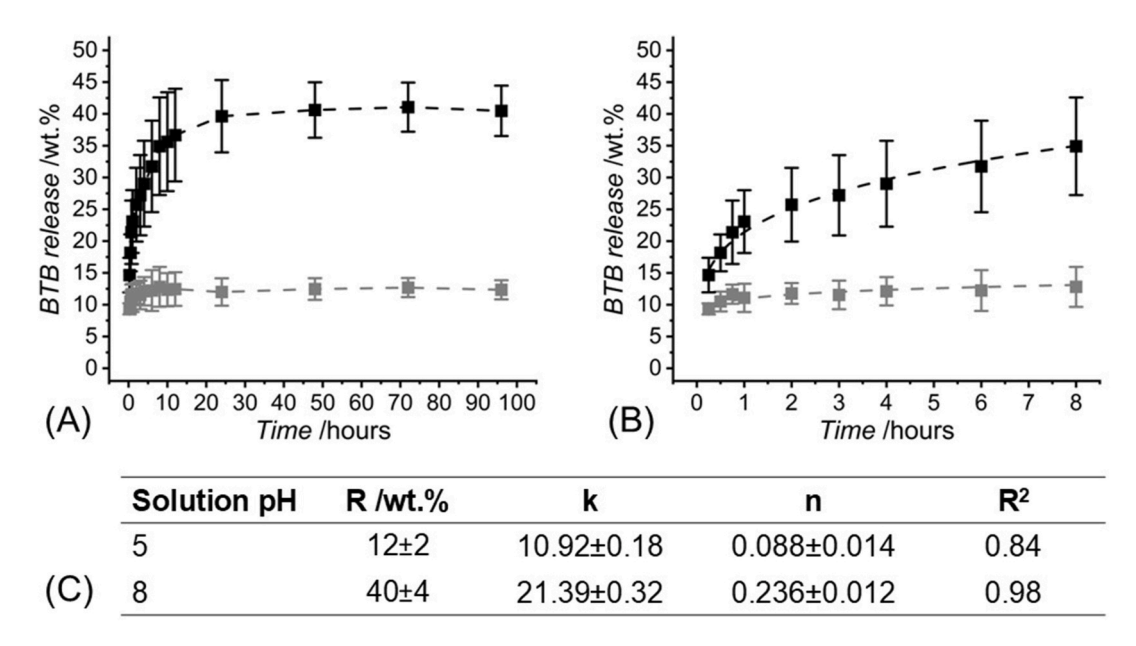
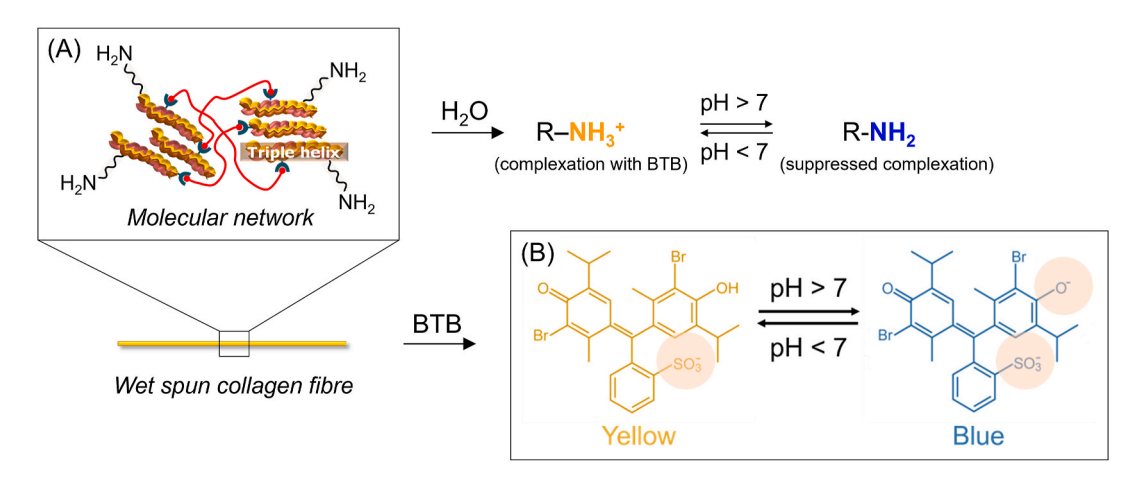


Fig. 6. BTB release measurements in acidic (pH 5, grey) and alkaline (pH 8, black) McIlvaine solutions. (A): Release profiles revealed by the BTB-loaded fibres following 96-h incubation. Lines are guidelines to the eyes. (B): Fitting of the first 60 % release data according to Korsmeyer-Peppas model ($y = k \cdot x^n$). (C): values of the 96-h release (R), Korsmeyer-Peppas model coefficients (k, n) and coefficient of determination (R^2) determined following incubation of drop cast fibres in either acidic (pH 5) or alkaline (pH 8) McIlvaine solutions. Data are presented as mean \pm standard deviation (n = 3).



Scheme 1. Proposed complexation mechanism underpinning the retention of BTB in the wet spun collagen fibre in aqueous environments. An increase in solution pH generates reversible protonation of the free amino groups of the UV-cured collagen network (A) and molecular reconfiguration of BTB towards an increased negative charge, as highlighted by the corresponding sulfonate and phenolate groups (B). Consequently, varying degree of electrostatic complexation between the dye and the collagen network can be expected.

the drop casting method employed in this study offers a compelling, low-cost and effective strategy for integrating wet-spun fibres with BTB retention capability in both acidic and alkaline environments, aiming to accomplish long-lasting halochromic capability for wound monitoring applications, without the need for particles or complex microstructures. The resulting high loading efficiency and supporting evidence of BTB-collagen electrostatic interactions suggest that this drop casting protocol also allows for the loading of tailored BTB dosages with minimal risks of abrupt, unwanted dye release and no cytotoxic effects from the UV-cured collagen materials [38,43,46,71].

While the encapsulation of pH-sensitive dyes prior to fibre production can alter polymer processability and lead to variations in fibre morphology and microstructure, the drop-casting method employed in this study enabled consistent loading of BTB onto the UV-cured hydrogel networks, whether in the form of wet-spun fibres or cast films [31]. The release profiles recorded with the drop cast fibres display no significant difference in alkaline conditions (pH 8; 12 h) in comparison to the thin films made of the same material, unlike the case when the same samples were incubated in acidic conditions (pH 5; 12 h). We hypothesise that the higher release observed from the fibres, as compared to the films, is due to the tightly packed and aligned molecular architecture of the wet-spun fibres, which may hinder dye absorption into the fibre core. The difference in material geometry may also contribute to this effect, given the microscale diameter of the wet-spun fibres relative to the millimetre-scale diameter of the collagen thin films.

Having confirmed dye release profiles in wound-relevant aqueous environments, attention was focused on assessing the colour-change functionality of the resulting BTB-loaded wet-spun collagen fibres (Table 2). The native fibres prior to drop casting exhibited a slight yellow hue (L = 68, C = 34, h = 87). Following dyeing with an aqueous BTB solution, a notable colour shift was recorded ($\Delta E \approx 27$), the colour

Table 2 Lightness (L), chroma (C), and hue (h) values for dry BTB-free fibres (F–4VBC*) and BTB-loaded fibres (B–4VBC*), as well as dried BTB-loaded fibres following 96-h incubation in McIlvaine solution at pH 5 and pH 8. Data are presented as mean \pm standard deviation (n = 9). The total colour difference (ΔE) is shown relative to BTB-loaded fibres as a single value for each sample (no SD). N/A: not applicable.

Sample ID	L	C	h	ΔΕ
F-4VBC*	68 ± 1	34 ± 1	87 ± 1	27
B-4VBC*	57 ± 2	52 ± 2	70 ± 2	N/A
B-4VBC* (96 h, pH 5)	43 ± 2	52 ± 3	61 ± 2	17
B-4VBC* (96 h, pH 8)	41 ± 2	20 ± 2	131 ± 2	70

became richer (C = 52) and slightly darker (L = 57), indicating substantial dye uptake and strong visible colouration, consistent with previously reported loading efficiency. After 96 h of incubation in acidic McIlvaine buffer (pH 5), only a moderate shift in the LCh colour coordinates was observed ($\Delta E \approx 17$), with hue and chroma largely preserved. This limited ΔE value suggests that the BTB remained mostly entrapped within the fibre matrix and retained its halochromic activity, indicating good dye robustness under prolonged aqueous conditions.

In contrast, immersion in alkaline McIlvaine solution (pH 8) resulted in a pronounced colour change ($\Delta E\approx 70$), shifting from yellow-orange to blue-green. This ΔE value approaches the theoretical maximum perceptual difference ($\Delta E\approx 100$) in the LCh colour space. This signifies a profound and unambiguous colour transition, far more than would occur from incidental fading, therefore making it highly detectable, even by non-experts. This substantial shift is consistent with the halochromic response of the embedded BTB and demonstrates clear pH-responsiveness of the fibre construct under alkaline conditions.

This colour change was demonstrated to be reversible and robust over clinically relevant time periods (Fig. 7). The fibres appeared bluegreen under alkaline conditions and consistently reverted to yellow-orange after multiple transfers into the acidic solution. Although the colour change capability of the fibres was demonstrated at room temperature only, it is likely that comparable behaviour would be observed at wound bed temperature, given the excellent thermal stability and consistent colour change capability of BTB at a temperature range of 25, 90 °C [72]

This pronounced and repeatable colour change under alkaline conditions highlights the suitability of the material for infection detection. This would allow clinicians and patients alike could visually monitor wound alkalinisation, a known early infection indicator [73] without the need for specialist instruments. The strong ΔE ensures robustness against changes in ambient lighting or moisture variability and supports potential smartphone-based or naked-eye monitoring of local pH.

Future work on colour measurements could encompass a broader range of pH values to yield a comprehensive spectral profile. The integration of these calibration datasets with smartphone-based colour analysis or dedicated mobile applications offers the potential for rapid, continuous and objective pH readouts at either the point of care or remotely. This methodology serves to complement the naked-eye monitoring demonstrated in the current feasibility study, aiming towards enhanced precision, reduced user subjectivity, and improved support for remote or self-managed wound monitoring.

Fig. 7. Photographs of BTB drop-cast collagen fibres displaying reversible colour change and durable infection-responsive capability over 96 h following alternating incubation steps in acidic (pH 5) and alkaline (pH 8) McIlvaine solutions. *Scale bars*: 10 mm. (For interpretation of the references to colour in this figure legend, the reader is referred to the Web version of this article.)

3.7. Wet-state tensile properties of UV-cured wet spun fibres

To evaluate whether the material retained mechanical competence in physiological environments, tensile testing was performed on both BTB-free and BTB-loaded collagen fibres after they reached equilibrium in PBS (Fig. 8). No statistically significant differences were observed in ultimate tensile strength (UTS), elongation at break (ϵ_b), or tensile modulus (E) between the two groups (Table 1), whose average values were measured as 12–15 MPa, 14–17 %, and 232–265 MPa, respectively. These findings suggest that any secondary molecular interactions between BTB and the collagen matrix did not translate into a measurable impact on bulk mechanical properties.

As shown in Fig. 8, the stress-strain curves of both BTB-free and BTB-loaded fibres displayed a similar profile, which was characterised by an initial, higher-stiffness, linear elastic region, followed by a transition to a lower-stiffness region. This yielding behaviour is likely associated with structural rearrangements, such as alignment of the collagen molecules in the direction of applied load or localised yielding of discrete domains [74,75]. The extent of yielding remains relatively limited, as evidenced by the modest deviation from linearity.

The subsequent lower-stiffness linear region may reflect the response of more compliant, hydrated zones within the covalently crosslinked collagen network.

Comparable manufacturing strategies have been reported in the literature to produce wet-spun collagen fibres with similar tensile strength and moduli under hydrated conditions. Notably, Pedro Kato

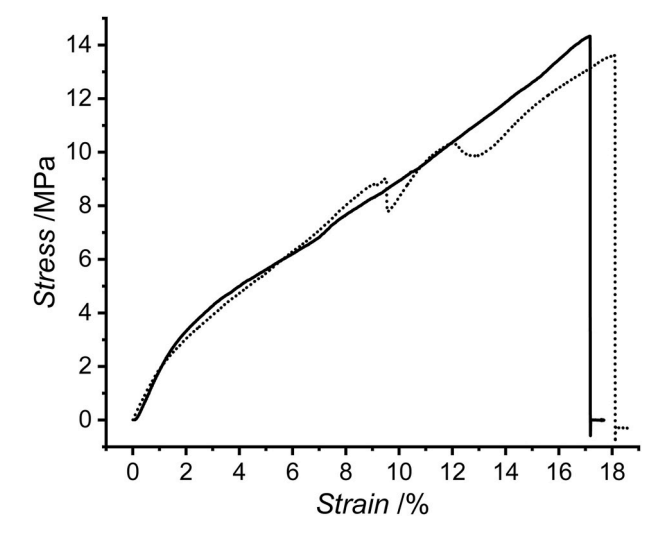


Fig. 8. Representative stress–strain curves (n=5) from uniaxial tensile tests performed on individual, UV-cured collagen fibres, either BTB-free (dotted line) or BTB-loaded (solid line), wet spun in a photoactive ethanol bath containing 0.5 wt% I2959. All fibres were incubated for 2 h in PBS (10 mM, pH 7.4) prior to testing.

et al. reported that fibres crosslinked via glutaraldehyde or through dehydration and cyanamide treatment exhibited enhanced tensile performance [76]. Glutaraldehyde-crosslinked fibres showed slightly higher tensile strength and modulus compared to those produced in this study, whereas comparable properties were measured with cyanamide-treated fibres (UTS: 24–31 MPa; E: 170–200 MPa). In another study, Tonndorf et al. developed wet-spun collagen yarns using a 6-hole spinneret followed by glutaraldehyde crosslinking, reporting a linear density of ca. 33 tex, a UTS of 40 \pm 4 MPa, and a Young's modulus of 281 \pm 15 [77] In contrast, the UV-cured wet-spun developed in this study exhibited a substantially lower linear density ($\lambda \approx 5$ tex), indicating superior mechanical integrity per unit mass.

Collagen extruded fibres have also been crosslinked via thermal dehydration at different temperatures (60, 80, 110, and 140 $^{\circ}$ C) and time intervals (1, 3, and 5 days). The crosslinked collagen fibres showed noticeably high UTS and elastic moduli in the dry state, exceeding 600 and 8000 MPa, respectively [78]. The magnitude of mechanical strength did not translate when fibres were hydrated, whereby a maximum value of UTS and moduli of ca. 92 and 90 MPa was observed, respectively. This value of UTS proved to be higher in comparison to the one measured in this study, an observation that is attributed to the significantly decreased fibre diameter than reported in this study. Significantly higher UTS was also recorded in collagen fibres crosslinked via either carbodiimide chemistry (UTS \approx 40 MPa) or glutaraldehyde (UTS \approx 138 MPa) [79], likely due to the application of fibre-drawing post-spinning.

Other than wet spinning, multifilament fibres were fabricated from blends of collagen and poly(ethylene oxide) (PEO) via contact drawing [80]. The reported mechanical properties (UTS $=24.79\pm4.07$ MPa; E $=344.3\pm0.0$ MPa) were comparable to those measured for the individual UV-cured collagen fibres developed in this study, despite the relatively modest swelling properties exhibited by the former samples.

The combination of remarkable wet-state tensile strength and reduced linear density supports the suitability of the UV-cured wet spun fibres as building blocks of textile-based wound dressings and highlights their suitability for use as lightweight, resorbable sutures. For instance, polypropylene 6-0 (PP) sutures have been reported to display a linear density comparable to that of the fibres produced in this study, but with significantly higher tensile modulus (E \approx 20 GPa) [81]. However, PP fibres lack biodegradability in physiological environments, necessitating the need for surgical removal following wound closure [81,82]. In contrast, the collagen fibres investigated here offer enzymatic degradability, presenting an appealing, patient-friendly alternative, while their tensile strength equips them with knot-forming and knot-tying abilities, further supporting their potential for suture applications (Section 3.8).

3.8. Fibre manufacturability onto woven dressings and resorbable sutures

Wet spinning of individual fibres is a well-established manufacturing process routinely employed by the textile industry for producing fibre-based healthcare materials such as wound dressings and implantable sutures. It was therefore of interest to investigate the scalability of the

manufacturing route developed here relative to industrial requirements.

Optimisation of our wet spinning apparatus led to a semi-automated extrusion setup, whereby the use of a 0.75 m coagulation bath allowed for the fabrication of fibres of up to 2.4 m in length (Fig. S3, Supp. Inf.). Due to the reduced mechanical integrity of freshly spun fibres, the extruded fibres were left in the coagulation bath for up to 10 min to enable complete collagen coagulation and minimise risks of fibre damage, prior to fibre collection onto the motorised spindle and UV curing (Scheme 2).

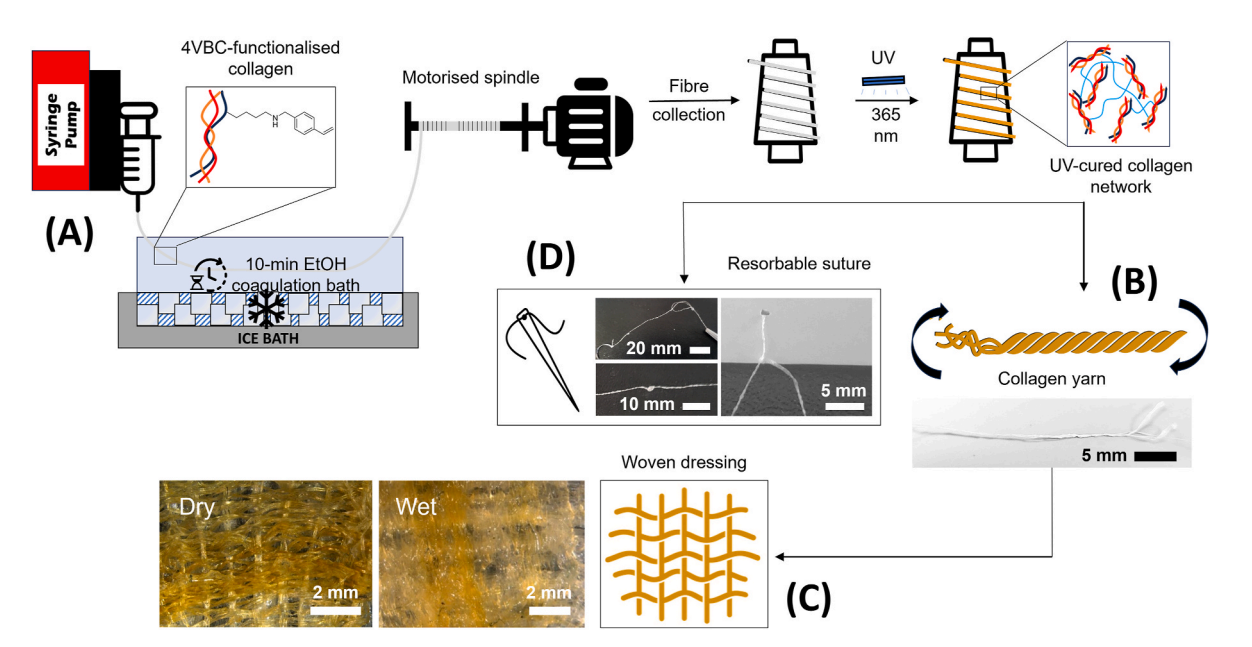
The application of low temperature (T = -20 °C) during fibre extrusion proved key to generate uniform fibres and minimise risks of collagen denaturation, as evidenced by FTIR analysis (Fig. 1). At the same time, the elongated shape of the coagulation bath enabled the reproducible manufacture of fibres with scalability to industrial manufacturing. The employment of a wet spinning dope with increased collagen concentration, together with an UV light system with improved spectral alignment, could provide an additional experimental space to further process automation and accomplish rapid in situ curing, damagefree fibre drawing and spooling. Nevertheless, the resulting UV-cured wet-spun fibres displayed sufficient mechanical competence to be successfully twisted into varns and subsequently woven into a dressing prototype, in line with current industrial manufacturing practices [83, 84]. The synthesis of a UV-cured molecular network proved therefore crucial for improving yarn compliance and minimising damage during handling, ultimately yielding a collagen-based textile dressing with integrated infection-responsiveness via colour-changing capabilities. Given the demonstrated fibre manufacturability, future work would be needed to investigate the BTB release profiles and pH-induced colour change capability described by the woven dressing prototype in use-inspired environments. Testing of the woven fabric will also be relevant to determine whether the larger volume of the corresponding collagen yarns (with respect to the wet spun fibres) leads to an increased retention of BTB.

Beyond their application in wound dressings, the elasticity and fineness of the UV-cured fibres supported their suitability as resorbable sutures, as evidenced by their ability to form and tie knots comparably to the case of commercial silk-braided sutures (Fig. S4, Supp. Inf.). For this application, however, further research is needed to assess the

biodegradability of the fibres in wound-simulated environments, whereby the material is applied on top of a simulated wound fluid layer rather than submerged in the solution, as carried out in this study. Ensuring delayed changes in mechanical properties during degradation will be essential to support the wound during the healing process and to minimise the risk of wound exposure to the external environment by degrading at the same rate as the wound healing process [63].

4. Conclusions

This study presents the design of individual pH-responsive textile fibres as building blocks of smart wound monitoring devices capable of reversible colour change in response to infection-associated alkaline shifts (pH $5 \rightarrow 7$). Scalable wet spinning of chemically functionalised type I collagen molecules was successfully integrated with UV-induced network formation and drop casting of pH-responsive bromothymol blue. The resulting drop-cast collagen fibres displayed an average thickness of 173 µm and an average dye loading efficiency of 99 wt%, enabling visual colour shifts when exposed to acidic (pH 5, $\Delta E = 17$) or alkaline (pH 8, $\Delta E = 70$) solutions. Wet spinning of the photoinitiatorloaded collagen dope in a 0.75 m coagulation bath vielded photoactive fibres of up to 2.4 m in length. Marginal increase in the coagulation bath absorbance following wet spinning $(0.000 \rightarrow 0.0007)$ indicated retention of the photoinitiator in the fibre-forming collagen jet, so that direct UV curing generated insignificant variations in gel content and mechanically competent fibres in the hydrated state. An average elongation at break, ultimate tensile strength, and tensile modulus of up to 17 %, 15 MPa, and 265 MPa were recorded, respectively. Knots could be tied in individual fibres, fibres twisted into yarns, and yarns woven into textile dressing prototypes which have been successfully demonstrated in vitro. More than a threefold increase in mass was observed following incubation and water-induced swelling of BTBloaded fibres in vitro. BTB was largely retained after 96 h submersion in either acidic (pH 5) or alkaline (pH 8) solutions, corresponding to an average release of 12 wt% and 40 wt%, respectively. This retention is attributed to the development of electrostatic interactions between the dispersed negatively charged BTB molecules and the primary amino groups present in the UV-cured collagen network, in line with the



Scheme 2. Scalable wet spinning of individual collagen fibres with enhanced mechanical competence. Fibres are extruded in an ethanol (EtOH) bath in contact with ice (A), and collected onto a motorised spindle, prior to UV curing and ethanol series dehydration. Resulting fibres can be twisted into yarns (B) to generate woven dressings (C) or used as resorbable suture with knot-forming and knot-tying abilities (D). The infection-responsive colour-change capability of the resulting products enables prompt infection diagnosis and tailored standards of care.

increased retention capability of the fibres in acidic environments. Following 24 h in a collagenase-rich medium, fibres retained up to ≈ 30 wt% of their initial mass. This finding supports the potential use of these UV-cured fibres as resorbable sutures. In light of their mechanical performance, infection responsivity, and scalable manufacturability, these multifunctional fibres offer broad applicability as wound monitoring devices, enabling prompt infection diagnosis and tailored standards of care, while maintaining compatibility and durability in the wound environment.

CRediT authorship contribution statement

Jonathon Gorman: Writing – review & editing, Writing – original draft, Visualization, Validation, Methodology, Investigation, Formal analysis, Conceptualization. Charles Brooker: Writing - review & editing, Writing - original draft, Visualization, Validation, Methodology, Investigation, Formal analysis, Data curation, Conceptualization. Xinyu Li: Methodology, Investigation, Formal analysis. Giuseppe Tronci: Writing - review & editing, Writing - original draft, Validation, Supervision, Resources, Project administration, Methodology, Funding acquisition, Data curation, Conceptualization.

Declaration of competing interest

G.T. is named inventor on a patent related to the fabrication of collagen-based materials. He has equity in and serves on the board of directors of HYFACOL Limited.

Acknowledgements

The authors gratefully acknowledge the financial support from Leeds Institute of Textile and Colour (LITAC) and the Clothworkers' Centre for Textile Materials Innovation for Healthcare (CCTMIH). The authors gratefully acknowledge Leeds Electron Miscroscopy And Spectroscopy centre (LEMAS) for their support and assistance conducting the SEM work. J.G. gratefully acknowledges the Whitworth Society for the financial support of his PhD program via the Senior Scholar Award. The authors would like to thank Mohammed Asaf (University of Leeds, School of Design) for technical assistance with TGA and DSC measurements.

Appendix A. Supplementary data

Supplementary data to this article can be found online at https://doi. org/10.1016/j.polymer.2025.129113.

Data availability

Data will be made available on request.

References

- [11] E. Sisli, A.A. Kavala, M. Mavi, O.N. Sariosmanoğlu, Ö. Oto, Single centre experience of combat-related vascular injury in victims of Syrian conflict: retrospective evaluation of risk factors associated with amputation, Injury 47 (9) (2016) 1945–1950.
- [2] K. Harding, D. Queen, Estimating the cost of wounds for the United Kingdom and its countries. Int. Wound J. 21 (2) (2024) e14616.
- [3] D. Oueen, K. Harding, Estimating the cost of wounds both nationally and regionally within the top 10 highest spenders, Int. Wound J. 21 (2) (2024) e14709.
- [4] L.R. Copeland-Halperin, A.J. Kaminsky, N. Bluefeld, R. Miraliakbari, Sample procurement for cultures of infected wounds: a systematic review, J. Wound Care 25 (Sup4) (2016) S4-S10.
- [5] E. Proksch, pH in nature, humans and skin, J. Dermatol. 45 (9) (2018) 1044–1052.
- [6] T. Maheswary, A.A. Nurul, M.B. Fauzi, The insights of microbes' roles in wound healing: a comprehensive review, Pharmaceutics 13 (7) (2021).
- [7] L.A. Schneider, A. Korber, S. Grabbe, J. Dissemond, Influence of pH on woundhealing: a new perspective for wound-therapy? Arch. Dermatol. Res. 298 (9) (2007) 413-420.

[8] F. Mariani, M. Serafini, I. Gualandi, D. Arcangeli, F. Decataldo, L. Possanzini, M. Tessarolo, D. Tonelli, B. Fraboni, E. Scavetta, Advanced wound dressing for realtime pH monitoring, ACS Sens. 6 (6) (2021) 2366-2377.

- [9] K. Kiti, C. Thanomsilp, O. Suwantong, The potential use of colorimetric pH sensor from Clitoria ternatea flower for indicating bacterial infection in wound dressing application, Microchem. J. 177 (2022) 107277.
- [10] Y. Li, S. Luo, Y. Gui, X. Wang, Z. Tian, H. Yu, Difunctional hydrogel optical fiber fluorescence sensor for continuous and simultaneous monitoring of glucose and
- [11] L. Manjakkal, D. Szwagierczak, R. Dahiya, Metal oxides based electrochemical pH sensors: current progress and future perspectives, Prog. Mater. Sci. 109 (2020)
- [12] D. Wencel, T. Abel, C. McDonagh, Optical chemical pH sensors, Anal. Chem. 86 (1) (2014) 15-29.
- [13] Q. Pang, F. Yang, Z. Jiang, K. Wu, R. Hou, Y. Zhu, Smart wound dressing for advanced wound management: real-time monitoring and on-demand treatment, Mater, Des. 229 (2023) 111917.
- [14] Y. Qin, H.-J. Kwon, M.M.R. Howlader, M.J. Deen, Microfabricated electrochemical pH and free chlorine sensors for water quality monitoring: recent advances and research challenges, RSC Adv. 5 (85) (2015) 69086-69109.
- [15] A. Gupta, S. Sharma, R. Goswami, Review-silicon based ISFETs: architecture, fabrication process, sensing membrane, and spatial variation, ECS J. Solid State Sci. Technol. 13 (4) (2024) 047006.
- [16] S. O'Callaghan, P. Galvin, C. O'Mahony, Z. Moore, R. Derwin, 'Smart' wound dressings for advanced wound care: a review, J. Wound Care 29 (7) (2020)
- [17] D.-K. Vo, K.T. Trinh, Advances in wearable biosensors for wound healing and infection monitoring, Biosensors (2025).
- [18] S. Chattopadhyay, R.T. Raines, Review collagen-based biomaterials for wound healing, Biopolymers 101 (8) (2014) 821-833.
- [19] S. Gajbhiye, S. Wairkar, Collagen fabricated delivery systems for wound healing: a new roadmap, Biomater. Adv. 142 (2022) 213152.
- [20] D.V. Verdolino, H.A. Thomason, A. Fotticchia, S. Cartmell, Wound dressings: curbing inflammation in chronic wound healing, Emerg. Top Life Sci. 5 (4) (2021) 523-537.
- [21] S. SenGupta, C.A. Parent, J.E. Bear, The principles of directed cell migration, Nat. Rev. Mol. Cell Biol. 22 (8) (2021) 529-547.
- [22] T.N. Demidova-Rice, A. Geevarghese, I.M. Herman, Bioactive peptides derived from vascular endothelial cell extracellular matrices promote microvascular morphogenesis and wound healing in vitro, Wound Repair Regen. 19 (1) (2011)
- [23] F. Revert-Ros, I. Ventura, J.A. Prieto-Ruiz, J.M. Hernández-Andreu, F. Revert, The versatility of collagen in pharmacology: targeting collagen. Targeting with Collagen, International Journal of Molecular Sciences, 2024.
- [24] S. Rýglová, M. Braun, T. Suchý, Collagen and its modifications—crucial aspects with concern to its processing and analysis, Macromol. Mater. Eng. 302 (6) (2017) 1600460.
- [25] H. Morris, R. Murray, Medical textiles, Textil. Prog. 52 (1-2) (2020) 1-127.
- [26] H. Morris, R. Murray, Medical Textiles, 2021, pp. 351–356.
 [27] M. Shahriari-Khalaji, A. Alassod, Z. Nozhat, Cotton-based health care textile: a mini review, Polym. Bull. 79 (12) (2022) 10409-10432.
- [28] T. Tat, G. Chen, X. Zhao, Y. Zhou, J. Xu, J. Chen, Smart textiles for healthcare and sustainability, ACS Nano 16 (9) (2022) 13301-13313.
- [29] N. Akombaetwa, A. Bwanga, P.A. Makoni, B.A. Witika, Applications of electrospun drug-eluting nanofibers in wound healing: current and future perspectives, Polymers (2022).
- [30] H. Kim, J.H. Kim, M. Jeong, D. Lee, J. Kim, M. Lee, G. Kim, J. Kim, J.S. Lee, J. Lee, Bioelectronic sutures with electrochemical pH-Sensing for long-term monitoring of the wound healing progress, Adv. Funct. Mater. 34 (40) (2024) 2402501.
- [31] H. Liang, J. Yin, K. Man, X.B. Yang, E. Calciolari, N. Donos, S.J. Russell, D.J. Wood, G. Tronci, A long-lasting guided bone regeneration membrane from sequentially functionalised photoactive atelocollagen, Acta Biomater. 140 (2022) 190-205.
- [32] L. Xu, Y. Liu, W. Zhou, D. Yu, Electrospun medical sutures for wound healing: a review, Polymers (2022).
- [33] W. Eom, H. Shin, R.B. Ambade, S.H. Lee, K.H. Lee, D.J. Kang, T.H. Han, Large-scale wet-spinning of highly electroconductive MXene fibers, Nat. Commun. 11 (1) (2020) 2825.
- [34] J. Xiong, P.S. Lee, Progress on wearable triboelectric nanogenerators in shapes of fiber, yarn, and textile, Sci. Technol. Adv. Mater. 20 (1) (2019) 837-857.
- [35] D.G. Dassanayaka, T.M. Alves, N.D. Wanasekara, I.G. Dharmasena, J. Ventura Recent progresses in wearable triboelectric nanogenerators, Adv. Funct. Mater. 32 (44) (2022) 2205438.
- [36] D.D. Pedersen, S. Kim, W.R. Wagner, Biodegradable polyurethane scaffolds in regenerative medicine: clinical translation review, J. Biomed. Mater. Res. 110 (8) (2022) 1460-1487.
- [37] L. Yang, H. Liu, S. Ding, J. Wu, Y. Zhang, Z. Wang, L. Wei, M. Tian, G. Tao, Superabsorbent fibers for comfortable disposable medical protective clothing, Adv. Fiber Mater. 2 (3) (2020) 140-149.
- C. Brooker, G. Tronci, A collagen-based theranostic wound dressing with visual, long-lasting infection detection capability, Int. J. Biol. Macromol. 236 (2023)
- [39] N. Rajan, J. Habermehl, M.F. Coté, C.J. Doillon, D. Mantovani, Preparation of ready-to-use, storable and reconstituted type I collagen from rat tail tendon for tissue engineering applications, Nat. Protoc. 1 (6) (2006) 2753-2758.
- [40] G. Tronci, S.J. Russell, D.J. Wood, Photo-active collagen systems with controlled triple helix architecture, J. Mater. Chem. B 1 (30) (2013) 3705-3715.

- [41] P. Cayot, G. Tainturier, The quantification of protein amino groups by the trinitrobenzenesulfonic acid method: a reexamination, Anal. Biochem. 249 (2) (1997) 184–200.
- [42] M. Vallecillo-Rivas, M. Toledano-Osorio, C. Vallecillo, M. Toledano, R. Osorio, The collagen origin influences the degradation kinetics of guided bone regeneration membranes, Polymers 13 (17) (2021).
- [43] G. Tronci, J. Yin, R.A. Holmes, H. Liang, S.J. Russell, D.J. Wood, Protease-sensitive atelocollagen hydrogels promote healing in a diabetic wound model, J. Mater. Chem. B 4 (45) (2016) 7249–7258.
- [44] Y. Liu, Q. Zheng, M. Tan, Z. Chen, H. Zheng, J. Gao, H. Lin, G. Zhu, W. Cao, Characterization and film-forming properties of collagen from three species of sea cucumber from the South China Sea: emphasizing the effect of transglutaminase, Int. J. Biol. Macromol. 294 (2025) 139321.
- [45] Y. Liu, D. Ma, Y. Wang, W. Qin, A comparative study of the properties and self-aggregation behavior of collagens from the scales and skin of grass carp (Ctenopharyngodon idella), Int. J. Biol. Macromol. 106 (2018) 516–522.
- [46] J. Yin, D.J. Wood, S.J. Russell, G. Tronci, Hierarchically assembled type I collagen fibres as biomimetic building blocks of biomedical membranes, Membranes 11 (8) (2021)
- [47] B.F. Far, M. Jahanbakhshi, L. Jameie, A. Shojaei, K. Zarei, P. Taromi, S. Jafarzadeh, Y.N. Ertas, Chitosan-graft-gelatin hydrogel containing bromothymol blue as a food spoilage indicator for intelligent food packaging, Adv. Mater. Interfac. 12 (9) (2025) 2400799.
- [48] T.U. Nguyen, K.E. Watkins, V. Kishore, Photochemically crosslinked cell-laden methacrylated collagen hydrogels with high cell viability and functionality, J. Biomed. Mater. Res. 107 (7) (2019) 1541–1550.
- [49] I. Mironi-Harpaz, D.Y. Wang, S. Venkatraman, D. Seliktar, Photopolymerization of cell-encapsulating hydrogels: crosslinking efficiency versus cytotoxicity, Acta Biomater. 8 (5) (2012) 1838–1848.
- [50] A.J. Finch, J.M. Benson, P.E. Donnelly, P.A. Torzilli, Light absorptive properties of articular cartilage, ECM molecules, synovial fluid, and photoinitiators as potential barriers to light-initiated polymer scaffolding procedures, Cartilage 10 (1) (2017) 82, 93
- [51] M.T. Arafat, G. Tronci, J. Yin, D.J. Wood, S.J. Russell, Biomimetic wet-stable fibres via wet spinning and diacid-based crosslinking of collagen triple helices, Polymer 77 (2015) 102–112.
- [52] M. Li, C. Brooker, R. Ambike, Z. Gao, P. Thornton, T. Do, G. Tronci, Photodynamic, UV-curable and fibre-forming polyvinyl alcohol derivative with broad processability and staining-free antibacterial capability, Eur. Polym. J. 228 (2025) 113794.
- [53] M. Yousefi, F. Ariffin, N. Huda, An alternative source of type I collagen based on by-product with higher thermal stability, Food Hydrocoll. 63 (2017) 372–382.
- [54] A.M. Mansour, M.K. Seddeek, Fabrication and characterization of bromothymol blue nanocrystalline films for potential optoelectronic applications, J. Inorg. Organomet. Polym. Mater. (2025).
- [55] M. Cadenaro, L. Fontanive, C.O. Navarra, P. Gobbi, A. Mazzoni, R. Di Lenarda, F. R. Tay, D.H. Pashley, L. Breschi, Effect of carboidiimide on thermal denaturation temperature of dentin collagen, Dent. Mater. 32 (4) (2016) 492–498.
- [56] M. Majeed, M.A. Rather, Valorization of rohu fish (Labeo rohita) skin waste into high-quality type-I collagen biomaterial: extraction, optimization, and characterization, Polym. Renew. Resour. 16 (2–3) (2025) 85–104.
- [57] G. Tronci, R.S. Kanuparti, M.T. Arafat, J. Yin, D.J. Wood, S.J. Russell, Wet-spinnability and crosslinked fibre properties of two collagen polypeptides with varied molecular weight, Int. J. Biol. Macromol. 81 (2015) 112–120.
- [58] M. Minsart, S. Van Vlierberghe, P. Dubruel, A. Mignon, Commercial wound dressings for the treatment of exuding wounds: an in-depth physico-chemical comparative study, Burns Trauma 10 (2022) tkac024.
- [59] X. Peng, G. Liu, L. Zhu, K. Yu, K. Qian, X. Zhan, In vitro and in vivo study of novel antimicrobial gellan–polylysine polyion complex fibers as suture materials, Carbohydr, Res. 496 (2020) 108115.
- [60] C. Vallecillo, M. Toledano-Osorio, M. Vallecillo-Rivas, M. Toledano, R. Osorio, biodegradation pattern of collagen matrices for soft tissue augmentation, Polymers (2021)

- [61] S.M. Ali, N.Y. Patrawalla, N.S. Kajave, A.B. Brown, V. Kishore, Species-based differences in mechanical properties, cytocompatibility, and printability of methacrylated collagen hydrogels, Biomacromolecules 23 (12) (2022) 5137–5147.
- [62] M. Meyer, Processing of collagen based biomaterials and the resulting materials properties, Biomed. Eng. Online 18 (1) (2019) 24.
- [63] A.T. Neffe, G. Tronci, A. Alteheld, A. Lendlein, Controlled change of mechanical properties during hydrolytic degradation of polyester urethane networks, Macromol. Chem. Phys. 211 (2) (2010) 182–194.
- [64] M.V. Ghica, M.G. Albu Kaya, C.-E. Dinu-Pîrvu, D. Lupuleasa, D.I. Udeanu, Development, optimization and in Vitro/In vivo characterization of collagendextran spongious wound dressings loaded with flufenamic acid, Molecules (2017).
- [65] W. McGuiness, E. Vella, D. Harrison, Influence of dressing changes on wound temperature, J. Wound Care 13 (9) (2004) 383–385.
- [66] S. Horiike, S. Matsuzawa, K. Yamaura, Preparation of chemically crosslinked gels with maleate-denatured poly(vinyl alcohol) and its application to drug release, J. Appl. Polym. Sci. 84 (6) (2002) 1178–1184.
- [67] J. Gong, Y.C. Ching, S. Huang, Q.J. Niu, A. Li, C.K. Yong, T.M.S.U. Gunathilake, N. Dai Hai, C.C. Hock, A dual stimuli-responsive cellulose-based double network hydrogel crosslinked with fluorescent carbon dots for controlled drug release, React. Funct. Polym. (2025) 106344.
- [68] M.B. Bazbouz, G. Tronci, Two-layer electrospun system enabling wound exudate management and visual infection response, Sensors (2019).
- [69] C. Wu, Y. Zhu, T. Wu, L. Wang, Y.I. Yuan, J. Chen, Y. Hu, J. Pang, Enhanced functional properties of biopolymer film incorporated with curcurmin-loaded mesoporous silica nanoparticles for food packaging, Food Chem. 288 (2019) 130-145
- [70] J. Zhang, Y. Yang, J. Zhang, J. Shi, L. Liu, X. Huang, W. Song, Z. Li, X. Zou, M. Povey, High-stability bi-layer films incorporated with liposomes@ anthocyanin/carrageenan/agar for shrimp freshness monitoring, Foods 12 (4) (2023) 732.
- [71] H. Hou, Y. Zhao, C. Li, M. Wang, X. Xu, Y. Jin, Single-cell pH imaging and detection for pH profiling and label-free rapid identification of cancer-cells, Sci. Rep. 7 (1) (2017) 1759.
- [72] N.M. Poovadichalil, A. Ullah, M.R. Maurya, A. Hasan, K.K. Sadasivuni, Eco-friendly paper-based colorimetric sensor for portable and rapid detection of lead (II) ions in aqueous environment, Int. J. Environ. Sci. Technol. (2025) 1–12.
- [73] R. Derwin, D. Patton, H. Strapp, Z. Moore, The effect of inflammation management on pH, temperature, and bacterial burden, Int. Wound J. 20 (4) (2023) 1118–1129.
- [74] A.A. Poundarik, P.C. Wu, Z. Evis, G.E. Sroga, A. Ural, M. Rubin, D. Vashishth, A direct role of collagen glycation in bone fracture, J. Mech. Behav. Biomed. Mater. 52 (2015) 120–130.
- [75] S. Bose, S. Li, E. Mele, V.V. Silberschmidt, Exploring the mechanical properties and performance of Type-I collagen at various length scales: a progress report, Materials (2022).
- [76] Y.P. Kato, D.L. Christiansen, R.A. Hahn, S.-J. Shieh, J.D. Goldstein, F.H. Silver, Mechanical properties of collagen fibres: a comparison of reconstituted and rat tail tendon fibres, Biomaterials 10 (1) (1989) 38-42.
- [77] R. Tonndorf, D. Aibibu, C. Cherif, Collagen multifilament spinning, Mater. Sci. Eng. C 106 (2020) 110105.
- [78] W. Ming-Che, G.D. Pins, F.H. Silver, Collagen fibres with improved strength for the repair of soft tissue injuries, Biomaterials 15 (7) (1994) 507–512.
- [79] A. Yaari, Y. Schilt, C. Tamburu, U. Raviv, O. Shoseyov, Wet spinning and drawing of human recombinant collagen, ACS Biomater. Sci. Eng. 2 (3) (2016) 349–360.
- [80] R. Rasouli, H. Yaghoobi, J. Frampton, A comparative study of the effects of different crosslinking methods on the physicochemical properties of collagen multifilament bundles, ChemPhysChem 25 (14) (2024) e202400259.
- [81] R.N. Saha, M. Datta Roy, S. Ghosh, Developing uniform surgical suture size between USP/EP and textile engineering numbering system, Indian J. Surg. (2025).
- [82] P.B. Dobrin, Some mechanical properties of polypropylene sutures: relationship to the use of polypropylene in vascular surgery, J. Surg. Res. 45 (6) (1988) 568–573.
- [83] M.T. Hossain, M.A. Shahid, M.G.M. Limon, I. Hossain, N. Mahmud, Techniques, applications, and challenges in textiles for a sustainable future, J Open Innov. Technol. Mark. Complex. 10 (1) (2024) 100230.
- [84] E. Mathiowitz, L.D. M, R.A. Hopkins, Wet spun microfibers: potential in the design of controlled-release scaffolds? Ther. Deliv. 4 (9) (2013) 1075–1077.